Measurement of Forces between Two Mica Surfaces in Aqueous Electrolyte Solutions in the Range 0-100 nm

By Jacob N. Israelachvili*† and Gayle E. Adams §

Research School of Physical Sciences†§ and Research School of Biological Sciences,† Institute of Advanced Studies, The Australian National University, Canberra, ACT 2600, Australia

Received 19*th July*, 1977

The main results and conclusions of experimental measurements of the forces between molecularly smooth mica surfaces in aqueous electrolyte solutions are as follows:

(1) The attractive van der Waals forces in the range 1-15 nm are largely independent of the type and concentration of the aqueous electrolyte solution. From ~1 to ~6.5 nm the forces are non retarded with a Hamaker constant of $(2.2 \pm 0.3) \times 10^{-20}$ J. Above ~6.5 nm retardation effects set in and the forces decay more rapidly with increasing separation. The refractive indices of water and aqueous solutions between two mica surfaces are within 1 % of bulk values for surface separations in the range 2-100 nm.

(2) In KNO_3 solutions (10^{-4}-10^{-1} mol dm^{-3}) the measured double-layer repulsive forces are well described by non-linear (exact) solutions to the Poisson–Boltzmann equation for two double-layers interacting at constant surface potential. The effective surface potentials remain constant both as the surfaces approach each other and as the concentration is changed, and are independent of pH in the range 5.5-7. In concentrated KNO_3 solutions (10^{-2}-10^{-1} mol dm^{-3}) the double-layer repulsions still decay roughly exponentially with distance but the mean exponential decay lengths are ~25 % higher than the theoretical values.

(3) In $Ca(NO_3)_2$ and $BaCl_2$ solutions the double-layer forces are much reduced from those in KNO_3 solutions, and are poorly described by theory. The mean exponential decay lengths are much lower, by 20-45 %, than the theoretical Debye lengths even in dilute (10^{-4}-10^{-3} mol dm^{-3}) solutions.

(4) The surface or boundary from which the double-layer forces arise (the Outer Helmholtz Plane) is not always at the mica–water interface but may initially be up to 2.5 nm farther out from each surface. The existence and extent of such boundaries varies from mica to mica. These boundaries are irreversibly shifted towards the mica–water interfaces as the two surfaces approach each other, and thus give rise to hysteresis effects.

(5) Apart from the normal van der Waals and double-layer forces there is also an additional repulsive force. This force is an *additional* force and not a *modification* of the double-layer force, since it is independent of the type and concentration of electrolyte. Its magnitude varies from mica to mica; in all cases where it has been observed it is roughly exponential, having a characteristic decay length of 0.95 ± 0.20 nm.

(6) At small separations (below ~5 nm) the attractive van der Waals forces often exceed the repulsive forces, and the surfaces then fall into strong adhesive contact at a separation of 0.0 ± 0.4 nm relative to contact in uncleaved mica. The adhesion energies of mica surfaces in contact are complex, and are not given by extrapolating the long-range van der Waals and double-layer interaction energies down to separations of the order of interatomic spacings.

1. INTRODUCTION

The DLVO theory of colloidal stability [1, 2] is predicated on the notion that two independent types of forces govern the long-range interaction between similar colloidal particles immersed in polar (especially aqueous) solutions: attractive van der Waals

forces and repulsive double-layer forces. The DLVO theory has been extensively tested and reviewed,[3-5] and there has been much theoretical progress in our understanding of both the van der Waals forces [6-9] and the double-layer forces [10, 11] that form the basis of the theory. More recently, the theory has made inroads into biocolloidal phenomena [12, 13] and has enjoyed some success in highlighting the forces involved in inter cellular and inter membrane interactions.[14, 15] It is fair to say that the DLVO theory has withstood the test of time and that it stands today as the only quantitative theory of the colloidal and biocolloidal sciences.

But that is not to say that all experiments on colloidal behaviour, or long-range forces, are readily accounted by the DLVO theory. In the few cases where long-range forces have actually been measured, agreement with the theory has not always been obtained, especially at surface separations below about 10 nm. Only in the case of measurements of the equilibrium thicknesses of soap films with varying salt concentration has there been reasonable agreement with the theory over a large distance regime [3, 16-19] (film thicknesses: 10-100 nm). On the other hand, the results of measurements of long-range forces between quartz plates in water have been quite different from theoretical expectations.[20] Even when reasonable agreement with theory has been obtained, as in studies of soap film thicknesses,[3] crossed metal fibre force-barrier measurements,[21] rubber against glass measurements,[22-24] montmorillonite swelling pressures,[25-27] and the thickness of water films on glass, mica and metals,[28, 29] the agreement has tended to be restricted to a narrow distance regime; unexpectedly large repulsions have often appeared at small distances, below about 10 nm—attributed to the existence of "adsorbed hydration sheaths" or "structured water layers" around the particles.[16, 28] These small distance repulsions are in marked contrast to the DLVO theory which predicts an ultimate attraction at very small separations.

In spite of the enormous theoretical advances made in our understanding of intermolecular forces, these persistent discrepancies, particularly at small separations, have not yet been satisfactorily explained. It is unlikely that the source of the trouble lies in some anomalous van der Waals force behaviour at small separations; for both experiment and theory have indicated that the long-range van der Waals law of force extends to the short distance regime.[7, 8, 30-33] In contrast, the theoretical basis and formulation of double-layer forces are model-dependent and much more tenuous at small separations; there are even theoretical problems at large separations, expecially for asymmetric electrolytes.[34]

The existence of long-range repulsions between surfaces in water due to structural ordering of the water molecules has long been recognized,[16, 28, 35-38] though there has been much disagreement over the years on whether the effective range of this modified structure is small (a few Ångstrom) or large (a few thousand Ångstrom).[35-39] A theoretical framework for analysing such forces has recently been proposed.[40-42]

We have constructed an apparatus for measuring forces as a function of separation between two surfaces immersed in a liquid.* In what follows we describe the apparatus and the experimental techniques adopted for measuring the forces between two molecularly smooth surfaces of mica in various aqueous electrolyte solutions in the range 100 nm down to contact (adhesive) separations. Initially, we did not know what to expect, especially in view of earlier force measurements involving silicates in water,[20, 25-27, 44, 45] where the results were not readily accountable by DLVO forces. However, it quickly became apparent that the forces we were measuring were indeed double-layer and van der Waals forces, albeit with deviations from theory. We,

* A short account of the experimental technique and some initial results were reported earlier.[43]

therefore, adopt the DLVO theory as our theoretical yardstick in the shadow of which all our results will be discussed and compared.

2. APPARATUS AND EXPERIMENTAL METHODS

GENERAL FEATURES OF APPARATUS

The apparatus is shown in plate 1 and schematically in fig. 1. It is conceptually similar to earlier models by Tabor, Winterton and Israelachvili used for measuring van der Waals forces between mica surfaces in air and in vacuum,[46] the optical properties of liquid and monomolecular films [47] and in adhesion and boundary friction studies.[48, 49] The forces measured are those between two crossed cylindrical sheets of mica, glued to two optically polished curved glass discs. The mica used was ruby muscovite, from Bihar, India.

All the metal parts of the apparatus have been machined from 304 or 316 stainless steels passivated in 30 % HNO_3 at 50°C for 30 min. The O rings and glass-disc holders were made from Teflon and Delrin. During an experiment the apparatus is filled with liquid so that the two mica surfaces are entirely immersed in liquid. The capacity of the box is about 350 cm^3. There are three stop-cock inlets and outlets for passage of liquids and air. A specially constructed flow-through pH cell can be fitted to one of these. At the left of the apparatus is a small sideplate which houses a platinum conductivity cell and a glass thermistor which protrude into the liquid.

Three aspects of the apparatus require description: first, how is the separation between the two mica surfaces *controlled*; second, how is the separation *measured*; third, how are the forces measured?

CONTROL OF SEPARATION

The separation between the two mica surfaces is controlled by a three-stage mechanism (see fig. 1): the upper micrometer driven rod may be moved up and down by use of a two-way stepping motor (Rapid-syn, model 23H-502) which allows positioning to an accuracy of about one micrometer. The lower micrometer-driven rod is moved by a similar motorized mechanism using a two-way synchronous motor (Philips, motor 9904 111 04-331) and operates through a differential spring mechanism: the double cantilever steel spring is about a thousand times stiffer than the helical spring, so that a one micrometer movement of the motor-driven rod is reduced to a one nanometer displacement between the two mica surfaces. The lower synchronous motor is also connected to a high precision linear resistance potentiometer which reads 20.641 ± 0.004 kΩ/revolution. The calibration of the resistance with respect to distance is done optically during an experiment, a typical value being 30.0 ± 0.6 nm $k\Omega^{-1}$, whence the movement of the two mica surfaces may be measured. Finally, a rigid piezoelectric crystal tube (Vernitron, PZT 16-24125-4) is employed which expands or contracts longitudinally by about 0.7 nm V^{-1} applied across the crystal walls. This non-mechanical fine control is used to position the two surfaces to better than 0.1 nm. A voltage ramp generator connected to the piezoelectric crystal may also be employed to offset any purely thermal or mechanical drifts of the two surfaces over short periods of time during which delicate measurements are being made.

MEASUREMENT OF SEPARATION (SEE ALSO APPENDIX 1)

The separation between the mica surfaces may be measured to within 0.1-0.2 nm by use of multiple beam interference fringes.[46, 47] During an experimental run the fringes are continually monitored in a spectrometer (Jarrell–Ash half-meter grating spectrometer, dispersion: 32.8 Å/mm). The fringes are employed for measuring the separations between the surfaces as well as the refractive index of the liquid medium between them; further, the shapes of the surfaces, and therefore their radii and any surface deformation, may also be monitored by these fringes.[46-48]

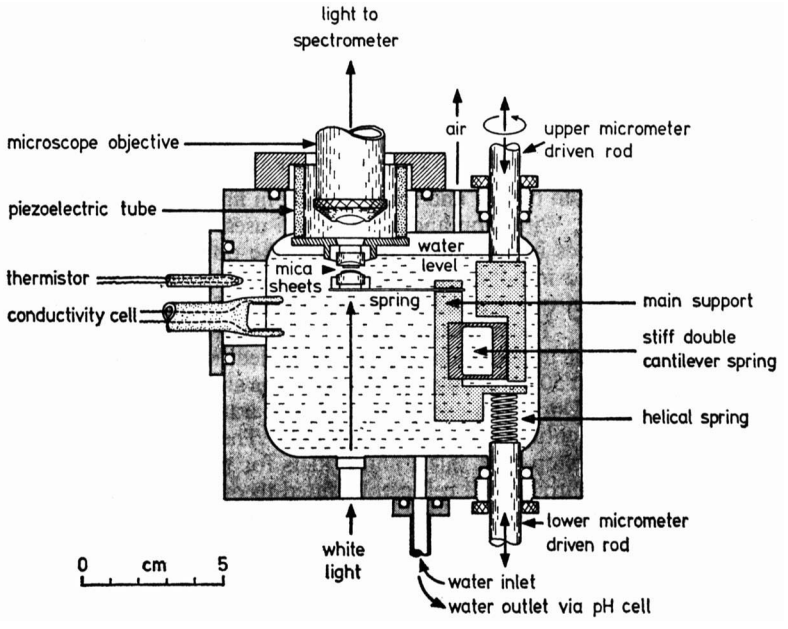

FIG. 1.—Schematic drawing of apparatus to measure long-range forces between two crossed cylindrical sheets of mica (of thickness ~1 μm and radius of curvature ~1 cm) immersed in liquid. By use of white light and multiple beam interferometry the shapes of, and separation between, the two mica surfaces may be independently measured. The separation between the two mica surfaces may be controlled by use of two micrometer-driven rods and a piezoelectric crystal tube to better than 0.1 nanometer. (Reproduced with some modifications from Nature [43] with permission).

METHODS OF MEASURING FORCES (SEE ALSO APPENDIX 2)

The glass disc supporting the lower mica sheet is suspended at the end of a steel cantilever leaf spring of stiffness $K \approx 10^2$ N m^{-1} (fig. 1). The forces are measured by suddenly reversing the voltage of the piezoelectric crystal, which expands or contracts it by a known (previously calibrated) amount. The resulting change in the separation between the two surfaces is then measured optically and any difference in the two values, when multiplied by the stiffness of the spring K, gives the force difference, whether attractive or repulsive, between the initial and final separations. The theoretical basis for this method is as follows: referring to fig. 2, let $x = 0$ define the zero (or laboratory reference) position of the lower surface when the two surfaces are a large distance apart and there is no interaction force between them.

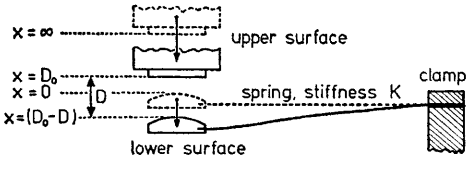

FIG. 2.—When two mica surfaces are at a distance D apart, the long range force between them $F(D)$ causes the spring to deflect by $(D-D_0)$ so that, at equilibrium, $F(D) = K(D-D_0)$. This equation forms the basis for the method of measuring the law of force $F(D)$.

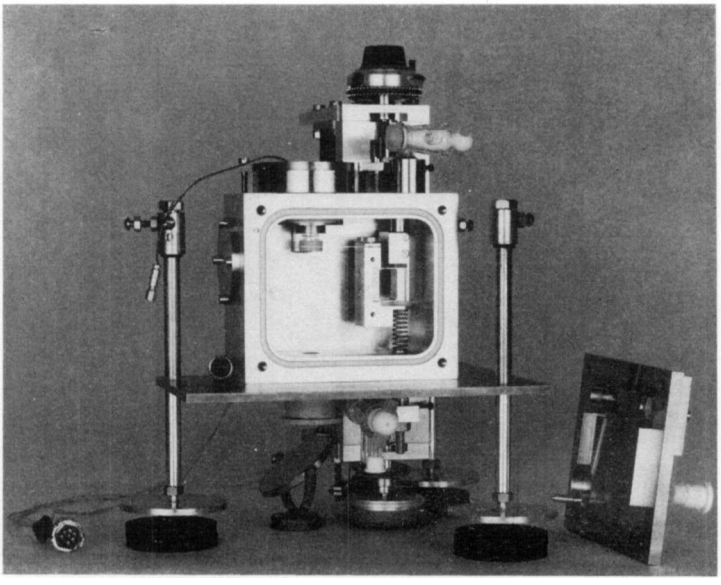

PLATE 1.—Apparatus (see fig. 1).

[*To face page* 978

As the upper surface is moved downwards to $x = D_0$ the interaction force between the surfaces causes the lower surface to move to a new equilibrium position at $x = -(D-D_0)$, *i.e.*, the spring deflexion is $(D-D_0)$. At any equilibrium surface separation D, the interaction force between the surfaces $F(D)$ is balanced by the restoring force of the spring $K(D-D_0)$, so that at equilibrium we have

$$F(D) = K(D-D_0) \tag{1}$$

where $F(D) > 0$ for repulsion.

Let the piezoelectric crystal expand by a finite amount ΔD_0, so that $D_0 \rightarrow D_0-\Delta D_0$, leading to a new equilibrium surface separation at $D-\Delta D$, then from eqn (1) we have

$$F(D-\Delta D) = K(D-\Delta D-D_0+\Delta D_0) = K(\Delta D_0-\Delta D)+F(D). \tag{2}$$

Eqn (2) shows that if an expansion of the crystal by an amount ΔD_0 causes the surfaces' separation to change by ΔD then the force difference between the initial position $F(D)$ and final position $F(D-\Delta D)$ equals $K(\Delta D_0-\Delta D)$. If $\Delta D_0 = \Delta D$ there is no force difference. Thus to measure the force $F(D)$ between the two surfaces using the optical technique we need only to know

(i) the leaf-spring stiffness, K. This is calibrated to within 1 % after each experiment by placing small weights at the place where the mica surfaces were contacting and measuring the deflection by a travelling microscope.

(ii) The amount the piezoelectric crystal expands or contracts, ΔD_0, when the voltage is reversed. This is measured optically at large separations where no forces are detected, before each run. The error in ΔD_0 is typically $\pm$(0.1-0.3) nm, and this contributes the major error in our quoted values of the " experimental Debye lengths ".

For example, if the surfaces are initially 100 nm apart, where there is no measurable force, and the crystal is expanded by 10 nm; then if the surfaces come to equilibrium at 90 nm there is, therefore, no force between the surfaces at 90 nm. However, if the two surfaces come to equilibrium at, say, 91 nm there is a repulsive force at 91 nm equivalent to bending the leaf-spring by 1 nm, *i.e.*, a force of $K(\Delta D_0-\Delta D) = 10^2(10\text{-}9)10^{-9} = 10^{-7}$ N. The time taken to reach equilibrium is about 1 s. By this method one can start at large separations, where no forces are detected, and work one's way down to smaller separations, and thus measure the force over any region of interest down to contact.

Over certain distance regimes (usually below 10 nm) the forces are often very large and rapidly varying with separation. In these regions of rapidly varying forces a second method of force measurement was found to be more suitable: in this method the lower surface is now moved by use of the lower rod, driven by the synchronous motor; in this way much larger displacements ΔD_0 may be attained than possible with the crystal. The displacements ΔD_0 are obtained from the change of resistance of the potentiometer as already described.

EXPERIMENTAL PROCEDURE

Before an experiment all parts of the apparatus are degreased, cleaned in dilute nitric acid, and washed in double distilled water. The mica sheets are prepared and mounted as described in earlier experiments.[46, 47] During experiments the apparatus is suspended from helical springs 1 m long inside a large wooden box. The helical springs partially isolate the apparatus from extraneous vibrations, though some residual vibration of the two surfaces (a few Ångstrom) was found to be an asset in that it indicated that the surfaces were truly separated and not contacting *via* an undetected dust particle or mica flake. Once the apparatus is suspended in the wooden box the surfaces are brought into molecular contact in air; the contact position is noted and the surfaces are then separated and the apparatus filled with a dilute aqueous electrolyte solution and allowed to settle for 1-2 h. The forces are then measured as described above. The electrolyte concentration is then increased by removing $\sim$30 cm^3 of solution from the lower stop-cock and injecting $\sim$30 cm^3 of a more concentrated solution through the front-plate stop-cock and mixing thoroughly by use of a syringe. The pH and conductivity of the solutions are usually measured at this point, and the 30 cm^3 of solution removed is kept for chemical analysis. This routine is repeated with a number of different concentrations. Sometime during a run the two

perpendicular radii of curvature, R_1 and R_2, of the surfaces are measured. The effective radius that is used in the plots of (F/R) against D is then (according to the Deryaguin approximation)[50] given by $R = \sqrt{R_1 R_2}$, and has a typical error of 5-10 %. On occasions measurements have also been made of the refractive index of the liquid medium and of the adhesion of the surfaces.

After an experimental fun the solutions were often checked for impurities by Atomic Absorption Spectroscopy (AAS) and assayed for organic carbon (Oceanography International, Model 0524 B-total carbon analyser). The double-distilled water from which the solution were made up had a typical specific conductance of $3 \times 10^{-6}\ \Omega^{-1}\ \mathrm{cm}^{-1}$. Its impurity content was typically: Na < 0.013, K < 0.1, Ca < 0.013, Si < 11, Fe < 0.1, Cr < 1.2, Al < 28, total organic carbon (excluding CO_2) < 8, all in μmol dm^{-3}. No inorganic impurities were ever detected in the dilute solutions (up to 10^{-2} mol dm^{-3}) except for small amounts of Na $\sim 2\ \mu$mol dm^{-3}. The carbon content varied from 2×10^{-4} mol dm^{-3} to below 8×10^{-6} mol dm^{-3} (detection limit) and appeared to come mainly from the apparatus itself and not from the original solutions. Analysis of the chemical compositions of the micas used in the experiments were carried out by Electron Microprobe Analysis as described in the literature.[51] In this technique a region approximately 1 μm wide and 1 μm deep is probed. The precision of the assays is: SiO_2($\pm$0.32 %), Al_2O_3($\pm$0.25 %), K_2O($\pm$0.13 %), Na_2O($\pm$0.1 %), MgO($\pm$0.1 %), FeO($\pm$0.1 %). There were significant variations in the compositions of the different micas used, and some sheets also exhibited minor local variations on scanning the surfaces. The mean compositions are given in the appropriate figure legends.

3. RESULTS

GENERAL FEATURES OF FORCES IN KNO_3 SOLUTIONS

Fig. 3 shows results obtained in KNO_3 solutions at 20°C, pH $\sim$ 6. For convenience we plot force/radius against distance (F/R against D), and note that according to the Derjaguin approximation [50] the corresponding interaction energy per unit area (energy/area) between two plane surfaces is equal to $F/2\pi R$. The repulsive forces were found to be exponential with decay lengths close to the Debye lengths, where

$$\text{Debye length} = \frac{1}{\kappa} = \left|\frac{\varepsilon \boldsymbol{k} T}{4\pi \sum_i n_i e_i^2}\right|^{\frac{1}{2}} = \frac{0.3045}{\sqrt{C}}\ \text{nm for a 1:1 electrolyte} \tag{3}$$

$$= \frac{0.176}{\sqrt{C}}\ \text{nm for a 2:1 electrolyte} \tag{4}$$

where C is the electrolyte concentration in mol dm^{-3}, $T = 20$°C, $\varepsilon = 80.1$ for water. (Note that the dielectric constants of aqueous electrolytes decrease linearly with increasing concentrations; but even for 0.1 mol dm^{-3} solutions the reduction in ε is at most 5 %).[52] A repeat experiment with a different pair of sheets taken from the same original mica sheet yielded identical results within experimental error (see experimental points with tails in fig. 3). One can readily fit the linear parts of the curves in fig. 3 to the well known approximate expression [ref. (2), p. 95, eqn (43)] for the repulsive double-layer interaction energy per unit area in 1 : 1 electrolyte (valid for distances greater than the Debye length):

$$\frac{\text{energy}}{\text{area}} = F/2\pi R = \frac{64nkT}{\kappa} \tanh^2 (e\psi/4kT)\, \mathrm{e}^{-\kappa D} \tag{5}$$

$$= (1.45 \times 10^{-11})\kappa \tanh^2 (\psi/101)\, \mathrm{e}^{-\kappa D}\ J\ \mathrm{m}^{-2} \tag{5a}$$

where ψ is the effective surface potential in mV.

For each of the concentrations in fig. 3 (excluding 1 mol dm^{-3}) a rough analysis using eqn (5) shows that the effective surface potential ψ remains fairly constant and close to 75 mV in the range 10^{-4}-10^{-1} mol dm^{-3} KNO_3. The inferred constancy of the surface potential at different KNO_3 concentrations implies that the effective surface charge density is roughly proportional to $\sqrt{C}$, and that (for $\psi \approx 75$ mV) it changes from about one electronic charge per 60 nm^2 in 10^{-4} mol dm^{-3} KNO_3 to one per 2 nm^2 in 10^{-1} mol dm^{-3} KNO_3. These effective surface charge densities are well below the maximum possible surface charge density of 1 charge per 0.5 nm^2 of a fully ionized mica surface.

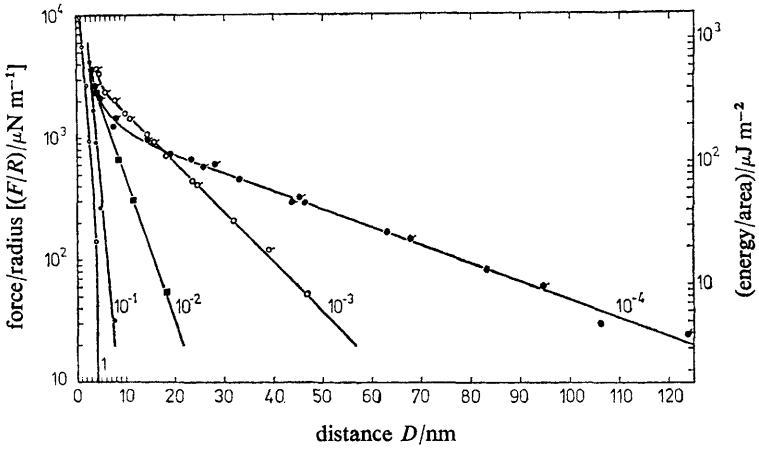

FIG. 3.—Experimental results of direct measurements of repulsive forces F (post-hysteresis) as a function of separation D between two crossed mica cylinders of radius R in aqueous KNO_3 solutions (concentrations marked in mol dm^{-3}). The right hand ordinate gives the interaction energy per unit area for two parallel plates, calculated according to the "Deryaguin approximation".[2, 50] The results in 10^{-4}-10^{-1} mol dm^{-3} solutions are for the same pair of mica sheets. The points with tails in 10^{-4} and 10^{-3} mol dm^{-3} solutions are for a different pair of sheets cut from the same sheet as the first pair. In 1 mol dm^{-3} KNO_3 the force was attractive above 4 nm (see fig. 4).

Subjecting the results of fig. 3 to closer scrutiny we find that within experimental error the exponential decay lengths, or slopes, of the lines in 10^{-4} and 10^{-3} mol dm^{-3} KNO_3 solutions are within 10 % of the theoretical Debye lengths, but in 10^{-2} and 10^{-1} mol dm^{-3} the slopes are about 20-25 % higher, while in 1 mol dm^{-3} the slope is ~250 % higher. (At separations below ~10 nm allowance has to be made for the effects of van der Waals forces before the double-layer forces and their slopes can be properly calculated. This is usually a small effect.) If we use eqn (5*a*) in which the values of κ are read off from the slopes of the lines, we obtain the following surface potentials: 82 mV at 10^{-4} mol dm^{-3}; 85 mV at 10^{-3} mol dm^{-3}; 62 mV at 10^{-2} mol dm^{-3}; 75 mV at 10^{-1} mol dm^{-3}, and 70 mV at 1 mol dm^{-3}. The error is about ± 10 mV. The slopes of fig. 3 are close to those obtained in other experiments. The mean values obtained for the ratio $\left(\frac{\text{measured exponential decay length}}{\text{theoretical Debye length}}\right)$ in various KNO_3 solutions are given below, together with the number of independent lines from which the mean values and their standard deviations were calculated, and the distance regimes over which the slopes were measured (normally 1-5 Debye lengths):

10^{-4} mol dm^{-3} : 0.96 ± 0.07 (9 lines, range 35-150 nm),

10^{-3} mol dm^{-3} : 1.03 ± 0.06 (6 lines, range 10-50 nm),

10^{-2} mol dm^{-3} : 1.25 ± 0.15 (5 lines, range 5-20 nm),

10^{-1} mol dm^{-3} : 1.20 ± 0.15 (4 lines, range 1-5 nm).

Similar results to those shown in fig. 3 were obtained in experiments with other pairs of mica sheets. Though different micas exhibited different surface potentials (varying between 50 and 130 mV) we found that these potentials remained constant, or that they decreased slightly, with increasing KNO_3 concentration. Further, the potentials were insensitive to pH in the range 5.5-7.0. It is worth looking into the compositional differences between the various micas used in these experiments in order to ascertain whether the surface potential is related to chemical composition. Below we tabulate the chemical compositions (in weight %) of some of the micas used, as determined by electron microprobe analysis, and their surface potentials (to within ± 10 mV) as determined from the double-layer forces :

SiO_2	Al_2O_3	FeO	MgO	TiO_2	Na_2O	K_2O	total	H_2O assumed	ψ/mV
46.37	35.77	1.43	1.12	0.2	0.83	10.55	96.27	3.73	60
46.07	35.65	1.54	0.95	—	0.81	10.58	95.60	4.40	80
46.14	37.64	0.82	0.34	—	0.97	10.10	96.01	3.99	100
46.17	37.59	0.95	0.52	—	0.96	10.17	96.36	3.64	110
45.94	37.29	0.96	0.56	—	0.93	10.14	95.81	4.19	130

Those micas which exhibited low surface potentials have significantly less Na and more K, and the amounts of Al, Fe and Mg also differ significantly. We may conclude that the bulk chemical composition appears to be related to the surface potential.

In 1 mol dm^{-3} KNO_3 solution the onset of repulsion was preceded by an attractive region, shown in fig. 4. In another experiment with different mica sheets whose surface potential was lower ($\psi \sim 50$ mV) an accurately measurable attractive region was also obtained in 10^{-1} mol dm^{-3} KNO_3 solution, also shown in fig. 4. At separations below these potential energy minima the repulsions rise very sharply. By extrapolating the exponential repulsive forces measured at smaller separations into the attractive force regimes it is possible to obtain fairly accurate estimates of the net attractive forces from about 4 nm upwards. These are shown as white circles in fig. 4 where we find that for the two entirely different experiments in 1 mol dm^{-3} and 10^{-1} mol dm^{-3} KNO_3 the net attractive forces coincide. We may conclude that these attractive forces are van der Waals dispersion forces, and that they have a non retarded Hamaker constant close to 2.2×10^{-20} J. The van der Waals forces are described more fully later.

Having described some of the gross features of the forces in KNO_3 solutions, we may conclude that, except for 1 mol dm^{-3} solutions, these are well described by the DLVO theory. But we have not yet described the behaviour at very small separations, below about 5 nm, where the forces were often quite different from those expected from the DLVO theory. Another feature of the measured forces was their hysteresis : the repulsion was often irreversibly reduced once the surfaces had been brought together closer than 2 nm ; but after the first close approach the (post-hysteresis) forces remained reversible and reproducible for many hours. In what follows we describe the results of further experiments in both 1 : 1 and 2 : 1 electrolytes in which individual items of data come together to reveal a comprehensive interaction

mechanism involving repulsive double-layer forces, attractive van der Waals forces, and an additional short distance repulsive force.

RESULTS IN 10^{-4} mol dm^{-3} KNO_3 AND 10^{-4} mol dm^{-3} $Ca(NO_3)_2$ SOLUTIONS

We begin with a more detailed description of the forces in 10^{-4} mol dm^{-3} solutions. These dilute concentrations are particularly suitable for testing the DLVO theory since (i) double-layer theory is expected to be valid, and (ii) the forces are large and extend over a large distance, which makes them amenable to accurate measurement and allows for detailed comparison with theory at separations below the Debye length.

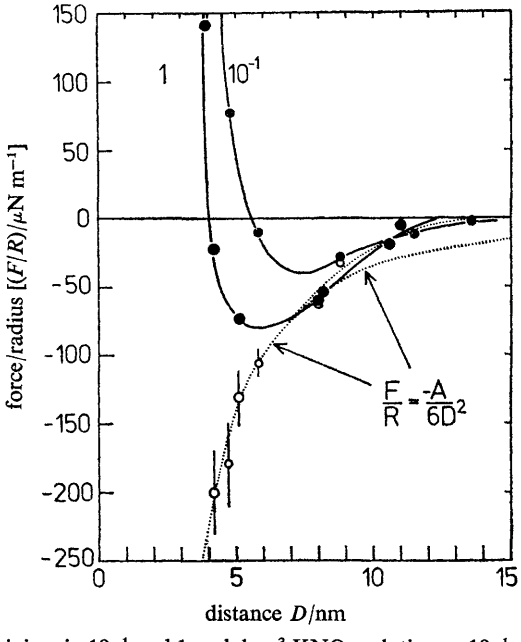

FIG. 4.—Secondary minima in 10^{-1} and 1 mol dm^{-3} KNO_3 solutions: 10^{-1} mol dm^{-3} (small circles), 1 mol dm^{-3} (large circles). By extrapolating the exponentially repulsive forces measured below 4 nm into the attractive force regimes one may obtain good estimates for the effective attractive forces above 4 nm. These are shown as open circles. Above about 8 nm these coincide with the measured forces. The upper dotted line shows the effective attractive force in the range 4-15 nm, which is the same for 10^{-1} and 1 mol dm^{-3} KNO_3 within experimental error. The lower dotted line shows a pure inverse square law of force, $F/R = A/6D^2$, corresponding to a purely non retarded van der Waals force of Hamaker constant $A = 2.2\times10^{-20}$ J. The two dotted lines coincide below ~7 nm but deviate at larger separations. Thus the attractive van der Waals forces are non retarded below ~7 nm, with a Hamaker constant of about 2.2×10^{-20} J. Above ~7 nm retardation sets in and the forces decay more rapidly.

10^{-4} mol dm^{-3} KNO_3

Fig. 5 shows detailed force against distance results in a $(1.07\pm0.03)\times10^{-4}$ mol dm^{-3} KNO_3 solution at 20.5 ± 0.5°C. The white circles are the pre-hysteresis forces, *i.e.*, those measured on the first approach. The black circles are the post-hysterests forces, *i.e.*, the forces measured subsequent to the first approach. The two results coincide, *i.e.*, there is no hysteresis. At 2.2 ± 0.3 nm the surfaces jumped into molecular contact (primary minimum). The concentration of the solution was checked

after the experimental run, and was found to contain K = 1.07×10^{-4}, Na < 10^{-8}, Ca < 10^{-8}, Si < 10^{-5}, Fe < 10^{-7}, Cr < 10^{-6}, organic carbon $\sim2\times10^{-5}$ all in mol dm^{-3}. In fig. 5 we have plotted the theoretical double-layer repulsion for 1.07×10^{-4} mol dm^{-3} 1 : 1 electrolyte, calculated by solving the non-linear Poisson–Boltzmann equation (see Appendix 2). This is shown as two solid curves for surfaces approaching at a constant potential of 130 mV (lower curve) and at constant charge (upper curve). If the theory is valid the experimental points should fall between these two limits.[10] The results indicate that the double-layer interaction is at constant potential below 10 nm.

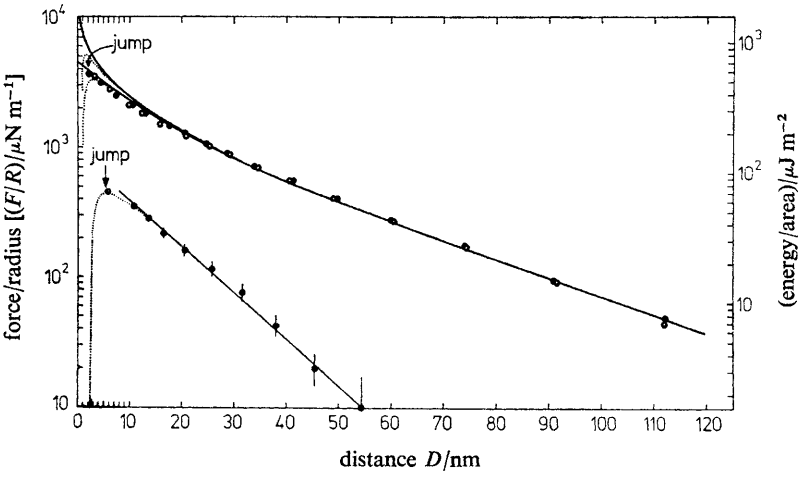

FIG. 5.—Measured forces in ○●, 1.07×10^{-4} mol dm^{-3} KNO_3 and ◐, 0.94×10^{-4} mol dm^{-3} $Ca(NO_3)_2$ between two mica sheets of composition (weight %): SiO_2 (45.94), Al_2O_3(37.29), FeO (0.96), MgO (0.56), Na_2O (0.93), K_2O (10.14). In 10^{-4} mol dm^{-3} KNO_3 the first and second (repeat) measurements are shown by open and closed circles respectively. At 2.2 nm the repulsion peaks and the surfaces jump into strong adhesive contact. The theoretical double-layer repulsions for a 1 : 1 electrolyte at constant potential and constant charge (for ψ = 130 mV at $D = \infty$) are shown by the lower and upper solid lines. The net theoretical DLVO forces, including the attractive van der Waals forces ($A = 2.2\times10^{-20}$ J), are shown as dotted lines. In 10^{-4} mol dm^{-3} $Ca(NO_3)_2$ the solid line is the best fit to the nine experimental points above 10 nm.

At 2.2±0.3 nm the surfaces jumped into contact (measured four times). These jumps took an estimated ¼-½ s. In Appendix 2 it is shown that jumps into contact occur once the repulsive forces have reached a peak and have just started to decrease. On coming into contact the surfaces deformed and assumed the characteristic flattened shapes of (initially) curves surfaces in strong adhesive contact, much like the shapes of contacting surfaces in air.[47, 48] These jumps into strong adhesive contact show that the repulsive forces not only decrease below 2.2 nm but that they rapidly become attractive.

In fig. 5 we have also added dotted lines which represent the net theoretical DLVO force F/R obtained by adding the non retarded van der Waals attractive force (with $A = 2.2\times10^{-20}$ J) to the double-layer repulsive forces. For constant potential the net repulsion peaks at about 3.0 nm, at which point the surfaces would be expected to jump into contact. For constant charge the jump should occur at about 1.5 nm. The measured jump at 2.2±0.3 nm implies either that there is some charge regulation at these small separations (*i.e.*, an interaction intermediate between constant charge and constant potential),[10] or that there is some additional repulsion below ~5 nm.

Within the framework of existing theories there exists yet another factor that may influence the turn about in the force: if the two surfaces have different potentials these could also account for the jumps.[11, 35] This may seem unlikely, especially since each pair of mica sheets was always cut from the same original sheet. Further, whenever jumps into contact were observed, these were always well accounted for by attractive van der Waals forces. However, we cannot rule out the possibility of small surface potential differences between the mica surfaces in our experiments.

Our assertion of distance determinations to within 0.1-0.2 nm requires some explanation. What is our " zero distance " or $D = 0$? In cases where the surfaces jumped into adhesive contact the distances D are referred to this contact, which defines $D = 0$. Once in contact, if the two surfaces are pressed further together by a large force, their contact area increases, but they do not come closer together. In cases where the surfaces repelled each other all the way, the contact ($D = 0$) values were obtained by pressing the surfaces together until no further approach was detectable. A series of tests on partially cleaved mica sheets (similar to those carried out by Tabor and Winterton [46]—see Appendix 1) indicated that contact separations in solution are at 0.0 ± 0.4 nm relative to that in uncleaved mica, which defines the $D = 0$ ordinate of all force against distance plots.

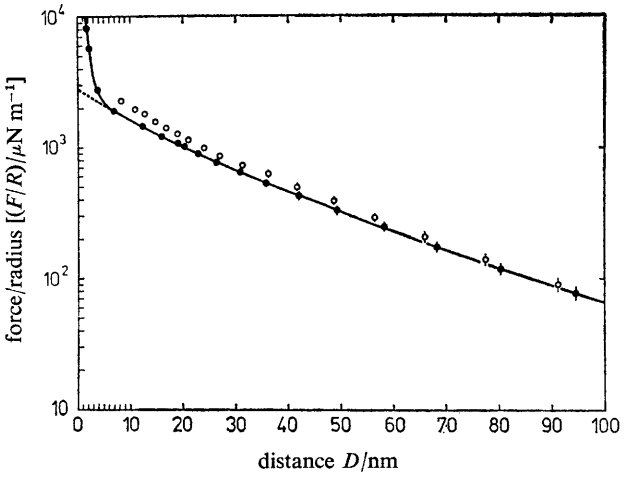

FIG. 6.—Measured forces in 1.00×10^{-4} mol dm^{-3} KNO_3 between two mica sheets of composition (weight %): SiO_2 (46.17), Al_2O_3 (37.59), FeO (0.95), MgO (0.52), Na_2O (0.96), K_2O (10.17). The first (pre-hysteresis) measurements are shown by open circles, the second (post-hysteresis) measurements by closed circles. The theoretical double-layer repulsion at a constant potential of $\psi = 110$ mV is shown by the solid line down to ~6 nm and the dashed line below ~6 nm.

We now describe the results of another experiment with different mica sheets in $(1.00 \pm 0.03)10^{-4}$ mol dm^{-3} KNO_3, shown in fig. 6. The open circles are the pre-hysteresis results (first approach), the closed circles are the reversible and reproducible post-hysteresis results. We immediately note two differences between these results and those shown in fig. 5: (1) there is hysteresis—the initial repulsive forces are larger than they are subsequently. (2) There is no jump into a primary minimum; instead, the forces become increasingly repulsive below about 6 nm. Above 6 nm the results are in agreement with theory for a double-layer interaction at a constant potential of 110 mV (solid line down to 6 nm, dashed line below 6 nm).

Hysteresis effects have long been known to occur in swelling pressure studies on clay sheets, notably between montmorillonite sheets in water,[25-27, 44] and it has been suggested that these are due to the forced alignment of edges or non-parallel sheets on the first compression. Since in our experiments no such edges exist in the region where the forces are being measured, it appears that the effect is a real one and not a bothersome artefact. Indeed, our experience with " edges ", which occur whenever the sheets tear up as sometimes happens after adhesive contact, is that once initiated these build up, rather than become smoothed out, with each additional approach and separation of the surfaces.

The hysteresis could be due to an irreversible neutralization or rearrangement of charges on the surfaces brought about by the first close approach; this would reduce ψ and the subsequent double-layer repulsion. Alternatively, the plane or boundary from which the diffuse double-layer repulsion originates (henceforth referred to as the Outer Helmholtz Plane, OHP) could be pushed in during the first compression, which would implicate a mechanism involving the breakdown of a structured aqueous domain at each surface. If the first explanation is correct, the post-hysteresis curve in fig. 6 has been moved down, while if the second is correct it has been moved to the left. If the surface potential has been reduced, then it has fallen by ~ 12 % from about 125 mV to about 110 mV; whereas if the OHP of each surface has been shifted, the inward displacement is about 2 nm (since the post- and pre-hysteresis results are displaced about 4 nm relative to each other along the distance axis). There is no way of telling which of these two explanations is correct (if either) without resorting to further experiments with different electrolyte concentrations.

As a test of whether there are structured aqueous regions near the surfaces, we measured the refractive index of the water between the two mica surfaces on the first approach and again subsequently. On the first approach the forces were not measured below 8 nm (hence the lack of experimental points below 8 nm in fig. 6); instead, the refractive index was measured. The values were all found to be within 1 % of the value for bulk 10^{-4} mol dm^{-3} KNO_3 solution ($\mu = 1.335$) down to a separation of about 2 nm. A repeat measurement after the first close approach yielded the same results. Thus if structured aqueous layers do exist near the mica surfaces their refractive index is very close to the value of bulk water.

The large additional repulsion observed at separations below 6 nm could be related to the hysteresis. Thus in fig. 5 there was no hysteresis and very little or no additional repulsion. But is the force below 6 nm an *additional* repulsion, or is it a *modification* of the double-layer force? We note that the additional repulsion is very large, and that below 3 nm it already exceeds the maximum possible repulsive force of a double-layer, whether at constant charge or potential [given by eqn (5) putting $\psi = \infty$]. The steep rise below 6 nm could be attributed to a dielectric constant of water near the interfaces different from the bulk value of 80. However, putting aside this speculation for the moment, and assuming that there exists an additional force below 6 nm, its magnitude in the range 1.5-6.0 nm can be obtained by subtracting the measured force from the expected double-layer force (dashed line). When this is done we obtain for the supposed additional force:

$$F/R = (44\,000 \pm 6000) \exp [-D/(0.85 \pm 0.05) \text{ nm}] \; \mu\text{N m}^{-1},$$

i.e., the additional force is roughly exponential with a characteristic decay length of 0.85 nm. If allowance is also made for the presence of van der Waals forces the additional force becomes

$$F/R = 41\,000 \exp (-D/0.95 \text{ nm}) \; \mu\text{N m}^{-1}.$$

The additional repulsion at small separations is not an artefact: whenever such repulsions were observed they were reproducible for different pairs of mica sheets cut from the same original sheet. This rules out the possibility that a stray particle had become lodged between the surfaces—an effect that would anyway be soon detectable either from the deformations of the fringes used to observe the surfaces and/or from the absence of vibrations. Why have the two different micas of fig. 5 and 6 interacted so differently at close separations (below 6 nm) while exhibiting almost identical forces, in agreement with double-layer force theory, at larger separations? The compositional difference of the two micas is not statistically significant (though it is worth noting that the results of electron microprobe analysis to a depth of $\sim 1\ \mu$m below the surface may be quite different from an analysis of the surface layers). We conclude from these and other experiments that while the bulk chemical composition appears to be related to the surface potential it has no apparent correlation with the hysteresis and additional repulsions at small separations. Finally, the values obtained for the surface potentials, and the magnitudes of the additional repulsive forces, did not depend on the relative orientation of the two mica sheets (since mica is birefrigent an orientation effect might be expected, but none was observed).

10^{-4} mol dm^{-3} $Ca(NO_3)_2$

Fig. 5 also shows results obtained in 0.94×10^{-4} mol dm^{-3} $Ca(NO_3)_2$ solution for the same pair of mica surfaces. We immediately note that the forces are much weaker than in 10^{-4} mol dm^{-3} KNO_3. A linear regression analysis of the 9 points above 10 nm of fig. 5 yields for the force law $F/R = (890 \pm 60) \exp(-D/12.2\ \text{nm})\ \mu\text{N m}^{-1}$ (solid line). The mean slope of the (assumed) exponential line in the range 10-55 nm is therefore 12.2 ± 1.0 nm, which is about 30 % less than the theoretical Debye length of 18.1 nm for a 2 : 1 electrolyte. At 5.3 ± 0.4 nm the surfaces jumped into contact. If we assume that non retarded van der Waals forces with a Hamaker constant of $A = 2.2 \times 10^{-20}$ J are also operating, then the total " theoretical " force should be $F/R = 890 \exp(-D/12.2\ \text{nm}) - A/6D^2$ (dotted line in fig. 5). In this experiment $R = 1.20$ cm, and the spring stiffness was $K = 1.33 \times 10^2$ N m^{-1}. At 5.0 nm the slope of the " theoretical " curve, $\partial F/\partial D$, equals K at which point the surfaces should jump into contact (Appendix 2). This agrees with the experimental jump distance of 5.3 ± 0.4 nm. At 2.2 nm the net force has fallen to zero, below which it rapidly becomes more attractive, eventually leading to strong contact adhesion. A more detailed analysis is possible, though probably unnecessary. Thus if we add 3×10^{-21} J to the measured dispersion Hamaker constant of 2.2×10^{-20} J to allow for the zero frequency contribution (as expected theoretically at distances below the Debye length)[7] we find that the increased van der Waals attraction, with $A = 2.5 \times 10^{-20}$ J, predicts a " theoretical " jump at 5.2 nm. But the experimental inaccuracy does not allow us to discriminate between these fine theoretical nuances. These results in 10^{-4} mol dm^{-3} $Ca(NO_3)_2$, as well as those in 10^{-4} mol dm^{-3} KNO_3, shows that the van der Waals forces are able to account for the observed peaks in the double-layer repulsions, and for the instability points at which the surfaces jump into contact.

Fig. 7 shows results with a different pair of mica sheets in various $Ca(NO_3)_2$ solutions. In 1.1×10^{-4} mol dm^{-3} $Ca(NO_3)_2$ above 6 nm the forces are similar to those shown in fig. 5. The slope of the line above 10 nm is 9.6 ± 0.6 nm, though when corrected for the van der Waals forces it becomes 9.2 ± 0.6 nm. This is about 45 % below the theoretical Debye length. The forces in 10^{-4} mol dm^{-3} $Ca(NO_3)_2$ of fig. 7 show the same type of unexpected repulsion below 6 nm that were found in

10^{-4} mol dm^{-3} KNO_3 (fig. 6). If, in fig. 7, we extrapolate the exponential " double-layer " force in 10^{-4} mol dm^{-3} $Ca(NO_3)_2$ below 6 nm, add to it the expected van der Waals force, and then subtract these from the measured total force, we find once again that there is an additional exponential repulsive force whose decay length is about 1.10 nm. This may be compared with the decay length of 0.95 nm previously obtained for the additional repulsive force below 6 nm in 10^{-4} mol dm^{-3} KNO_3.

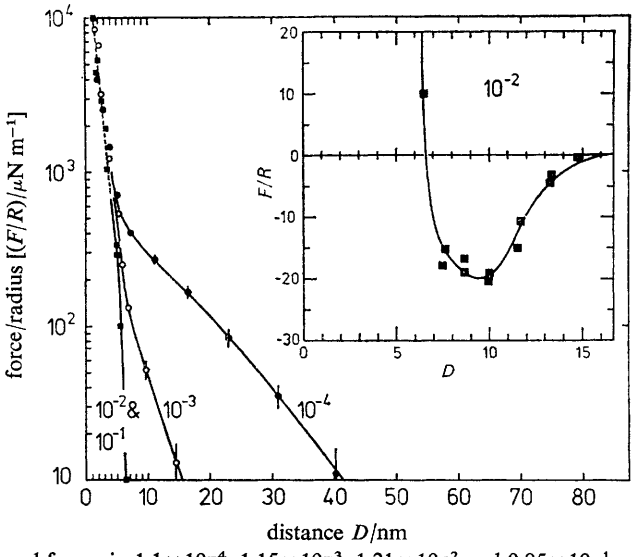

FIG. 7.—Measured forces in 1.1×10^{-4}, 1.15×10^{-3}, 1.21×10^{-2} and 0.95×10^{-1} mol dm^{-3} $Ca(NO_3)_2$ solutions (marked on curves) between two mica sheets of composition (weight %): SiO_2 (45.81), Al_2O_3 (37.60), FeO (1.00), MgO (0.43), Na_2O (1.04), K_2O (10.18). The results in 10^{-2} and 10^{-1} mol dm^{-3} $Ca(NO_3)_2$ were the same within experimental error. There was no hysteresis.

RESULTS AT HIGHER ELECTROLYTE CONCENTRATIONS (10^{-3}-10^{-1} mol dm^{-3})

Having described some of our results in 10^{-4} mol dm^{-3} 1 : 1 and 2 : 1 electrolyte solutions in some detail, and having introduced the effects of hysteresis and additional repulsions, we now continue with a description of results at higher concentrations.

Returning to fig. 7, in 1.15×10^{-3} mol dm^{-3} $Ca(NO_3)_2$ the exponential forces above 6 nm decay with a slope of 3.4 nm (or 3.0 nm when corrected for the van der Waals forces). This is about 40 % less than the theoretical Debye length. In another experiment in 10^{-3} mol dm^{-3} $Ca(NO_3)_2$ a value 45 % less than the theoretical Debye length was obtained. Thus for both 10^{-4} and 10^{-3} mol dm^{-3} $Ca(NO_3)_2$ we find that the exponential slopes are 0.6 ± 0.1 of the theoretical Debye lengths. Below 6 nm the force in 10^{-3} mol dm^{-3} $Ca(NO_3)_2$ rapidly increases and, as in 10^{-4} mol dm^{-3} $Ca(NO_3)_2$, becomes exponentially repulsive with a decay length of 0.95 ± 0.10 nm. The results in 10^{-2} and 10^{-1} mol dm^{-3} $Ca(NO_3)_2$ were practically the same: below 15 nm the forces were attractive (fig. 7 inset) and below 6.5 nm exponentially repulsive with a decay length of 1.0 ± 0.1 nm. The attractive van der Waals forces were very similar to those measured in 10^{-1} and 1 mol dm^{-3} KNO_3 solutions.

Our results in $Ca(NO_3)_2$ solutions show that at all the concentrations studied ($10^{-4}\rightarrow10^{-1}$ mol dm^{-3}) the forces below 6 nm approached the same limiting exponential repulsion (dashed line in fig. 7) given by

$$F/R = (50\,000\pm10\,000)\exp[-D/(1.00\pm0.15)\text{ nm}]\ \mu\text{N m}^{-1}.$$

This additional force is therefore independent of the electrolyte concentration and thus unlikely to be a modified double-layer repulsion. If the van der Waals forces are still operating as expected, with a Hamaker constant of $A \approx 2.2 \times 10^{-20}$ J then the net force should be given by $F/R = 50\,000 \exp(-D/1.0\text{ nm}) - A/6D^2$. In this experiment the value of R was 0.63 cm, and the spring consant $K = 1.30 \times 10^2$ N m^{-1}. Thus we should expect the surfaces to jump into contact when $\partial F/\partial D = K$, *i.e.*, at $D = 0.65 \pm 0.10$ nm. Normally, we would not bring the two surfaces so close during a force measurement since, once the repulsion F/R exceeds 8×10^3 μN m^{-1}, they begin to flatten because of the large repulsive forces. This does not invalidate any measurements made when flattening occurs, but it certainly complicates their interpretation.[22-24] In 10^{-1} mol dm^{-3} $Ca(NO_3)_2$ (fig. 7) we found that at $D = 1.10 \pm 0.05$ nm, and $F/R \approx 2 \times 10^4$ μN m^{-1}, the surfaces jumped into a strong adhesive contact. This jump distance was very reproducible, even after 15 h. The discrepancy between the expected jump distance of 0.65 nm and the measured jump distance of 1.10 nm is significant. However, if as a consequence of flattening the two surfaces locally appear more as two planes than as two crossed cylinders, the effective force between them would be proportional to $\partial(F/2\pi R)/\partial D$, where $F/R = 50\,000 \exp(-D/1.0\text{ nm}) - A/6D^2$ as before; the jump condition $\partial^2(F/2\pi R)/\partial D^2 = 0$ now occurs at 1.05 ± 0.10 nm in agreement with the measured value. This shift in the jump distance is a consequence of the Deryaguin approximation, as discussed in Appendix 2.

We may conclude that even in the presence of additional forces, the van der Waals forces are still operating at 1 nm separations with a Hamaker constant close to that measured at larger separations.

Two further tests were carried out to ensure that the additional forces were not an artefact. First, another experiment was performed in 10^{-4}-10^{-1} mol dm^{-3} $Ca(NO_3)_2$ using another pair of mica sheets cut from the same original sheet. The measured double-layer forces were very similar to those in fig. 7 at all four concentrations, and the additional repulsive forces were also of the same magnitude, with a mean decay length in the range 2-6 nm close to 1.0 nm. Second, the refractive index of the 10^{-1} mol dm^{-3} $Ca(NO_3)_2$ solution was measured in the range 1.1-100 nm. The results showed no deviation from the bulk value (1.3375) at any separation. The mean value of 34 readings was 1.339 ± 0.006.

Fig. 8 shows accurate results obtained in $(1.03 \pm 0.03) \times 10^{-3}$ mol dm^{-3} KNO_3 and $(1.08 \pm 0.02) \times 10^{-2}$ mol dm^{-3} KNO_3 solutions. The results at large separations are similar to those of fig. 3. In 10^{-3} mol dm^{-3} KNO_3 the double-layer repulsion in the range 4-50 nm agrees with theory for two surfaces approaching at a constant potential of $\psi = 100$ mV (lower solid line). There was no hysteresis, and some additional repulsion below 3 nm. At very small separations ($D < 0.6$ nm) the surfaces came into weak adhesive contact (primary minimum), though a clear jump into contact could not be measured. In 10^{-2} mol dm^{-3} KNO_3 the results are qualitatively similar, though the double-layer repulsion does not quite agree with theory (*cf.* solid line, representing the theoretical double-layer repulsion for $\psi = 50$ mV). The mean exponential slope in 10^{-2} mol dm^{-3} KNO_3 in the range 5-25 nm is 25-30 % *higher* than the theoretical Debye length. This deviation contrasts with that found for $Ca(NO_3)_2$ solutions where the exponential slopes are *lower* than the Debye lengths.

It should come as no surprise that in 10^{-2} mol dm^{-3} KNO_3 solutions the measured double-layer repulsion does not exactly agree with a theory that is valid only for very dilute solutions. What is intriguing is that in $Ca(NO_3)_2$ solutions large deviations from theory are already evident at 10^{-4} mol dm^{-3}, and that they are in opposite direction from those in KNO_3 solutions. In order to test whether the deviations in

$Ca(NO_3)_2$ are peculiar to $Ca(NO_3)_2$, or whether they might reflect a general property of 2 : 1 electrolytes, we carried out a series of force measurements with a completely different 2 : 1 electrolyte: $BaCl_2$. In 10^{-4} mol dm^{-3} $BaCl_2$ the mean exponential slopes of two independent measurements in the range 12-60 nm were 0.76 ± 0.06 and 0.79 ± 0.06 of the theoretical Debye lengths. In 10^{-3} mol dm^{-3} $BaCl_2$ the slopes were 0.56 ± 0.05 and 0.53 ± 0.06 of the theoretical Debye lengths. These deviations are in the same direction, though not as large, as those measured in 10^{-4} and 10^{-3} mol dm^{-3} $Ca(NO_3)_2$ solutions, and we are tempted to conclude that 2 : 1 electrolytes appear not to obey the Poisson–Boltzmann equation already at concentrations as low as 10^{-4} mol dm^{-3}.

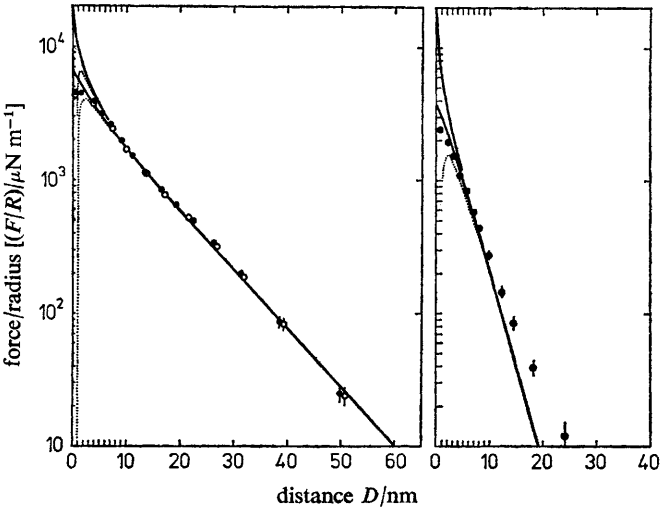

FIG. 8.—Left: Measured forces in 1.03×10^{-3} mol dm^{-3} KNO_3 between two mica sheets of composition (weight %): SiO_2 (46.14), Al_2O_3 (37.64), FeO (0.82), MgO (0.34), Na_2O (0.97), K_2O (10.10). The first and second (repeat) measurements are shown by open and closed circles respectively. Theoretical double-layer repulsions for a 1 : 1 electrolyte at constant potential and constant charge (for $\psi = 100$ mV at $D = \infty$) are shown by the lower and upper solid lines. The net DLVO interaction forces, including the attractive van der Waals forces ($A = 2.2 \times 10^{-20}$ J), are shown as dotted lines. These results were obtained at pH 6.95. A third series of force measurements at pH 5.35 yielded identical results within experimental error, but at pH 2.7 the repulsion was reduced by more than an order of magnitude. Right: Measured post-hysteresis forces in 1.08×10^{-2} mol dm^{-3} KNO_3 between two mica sheets of composition (weight %): SiO_2 (46.37), Al_2O_3 (35.77), TiO_2 (0.20), FeO (1.43), MgO (1.12), Na_2O (0.83), K_2O (10.55). The solid lines are the theoretical double-layer repulsions for a 1 : 1 electrolyte at constant potential (lower line) and constant charge (upper line) for $\psi = 50$ mV at $D = \infty$.

We have already shown (fig. 6) how double-layer forces were irreversibly reduced after the first approach of two surfaces in 10^{-4} mol dm^{-3} KNO_3. The decrease in the repulsion could have been due either to a reduction of the surface potential or to an inward shift of the OHP during the first approach. Fig. 9 shows results obtained in 1.0×10^{-1} mol dm^{-3} KNO_3 and 1.02×10^{-3} mol dm^{-3} $BaCl_2$ solutions (two separate experiments) in which large hysteresis effects were observed. In 0.1 mol dm^{-3} KNO_3 the first (pre-hysteresis) force is exponentially repulsive in the range 10-17 nm, with a decay length of 1.15 ± 0.10 nm. This is about 20 % higher than the theoretical Debye length, and is similar to the deviation observed in 10^{-2} mol dm^{-3} KNO_3 solutions. When we attempt to extract the effective surface potential

(or surface charge density) for the pre-hysteresis double-layer force we find that it is greater than infinity, *i.e.*, the measured force is well above the maximum theoretical double-layer force, given by eqn (5) for $\psi = \infty$. Thus if the measured pre-hysteresis force in 0.1 mol dm^{-3} KNO_3 is a true double-layer force then the $D = 0$ distance axis in fig. 9 must be shifted to $D \approx 5$ nm for the effective surface potential to be finite, *i.e.*, the OHP must be at least 2.5 nm beyond each mica surface. The post-hysteresis forces in 0.1 mol dm^{-3} KNO_3 (second and third data points in fig. 9) were measured 1 h and 2½ h respectively after the first approach. These reversible and reproducible post-hysteresis forces are well described by double-layer theory for two surfaces of surface potential $\psi \approx 75$ mV at $D = 0$ (or $\psi < 75$ mV if the post-hysteresis OHP is still at a finite distance from each mica surface, or if there is some additional force which has a similar decay length). We conclude that a reduction in the effective surface potential on the first approach cannot explain the observed hysteresis, and that an inward shift of the OHP is consistent with the observations.

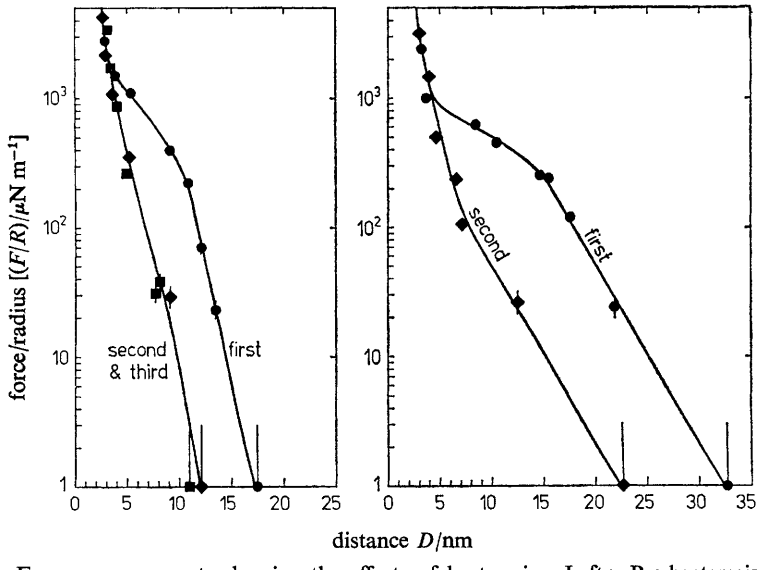

FIG. 9.—Force measurements showing the effects of hysteresis. Left: Pre-hysteresis forces (first approach) and post-hysteresis forces (second and third approaches) in 0.1 mol dm^{-3} KNO_3 between two mica sheets of composition (weight %): SiO_2 (46.42), Al_2O_3 (38.00), FeO (0.85), MgO (0.42), Na_2O (1.00), K_2O (10.15). Right: Hysteretic forces in 10^{-3} mol dm^{-3} $BaCl_2$ between two mica sheets of composition (weight %): SiO_2 (46.49), Al_2O_3 (35.46), FeO (1.36), MgO (1.01), TiO_2 (0.20), Na_2O (0.69), K_2O (10.57).

Fig. 9 also shows hysteresis in 1.02×10^{-3} mol dm^{-3} $BaCl_2$ solution. At large separations the pre-hysteresis and post-hysteresis forces (first and second data points) have the same exponential decay length of ~3.0 nm, *i.e.*, ~55 % of the theoretical Debye length, similar to that obtained for 10^{-3} mol dm^{-3} $Ca(NO_3)_2$. At small separations, below 5 nm, both forces tend to the same limiting exponential repulsion of decay length ~1.0 nm, characteristic of the existence of additional repulsive forces. The post-hysteresis force in 10^{-3} mol dm^{-3} $BaCl_2$ is very similar at all separations to the force in 10^{-3} mol dm^{-3} $Ca(NO_3)_2$ shown in fig. 7.

Large hysteresis has also been observed in a 1 mol dm^{-3} KNO_3 solution. In one experiment the pre-hysteresis force was repulsive all the way down to 1.5 nm

separations; the post-hysteresis repulsion was much reduced and exposed a deep secondary minimum (see fig. 3 and 4), and was reproducible 15 h later. Hysteresis effects were also observed in other experiments with KNO_3 and $BaCl_2$ solutions; these were weaker than those already described but had the same general features. Hysteresis effects were rarely observed in dilute solutions. Increasing the electrolyte concentration can bring about hysteresis.

VAN DER WAALS FORCES

The attractive van der Waals forces have been studied in two ways. At high electrolyte concentrations, when double layer repulsions are weak, the attractive forces may be measured in the region of a secondary minimum, as described earlier.

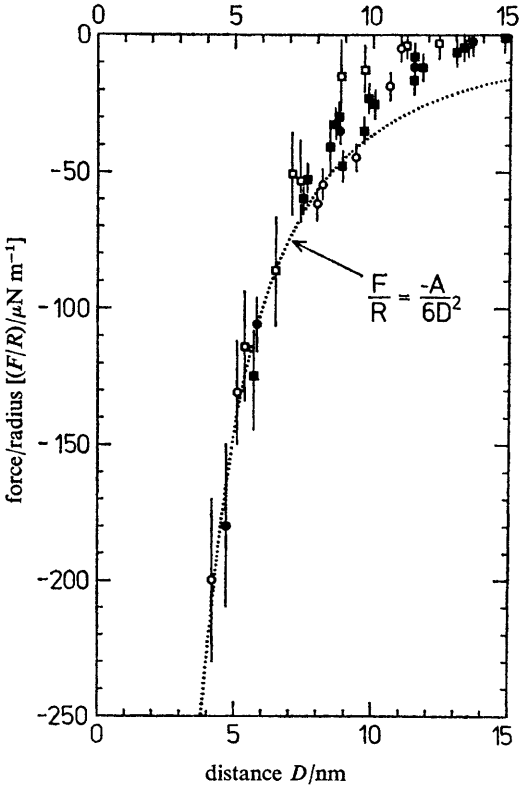

FIG. 10.—Attractive van der Waals dispersion forces between mica surfaces measured in the region of secondary minima in various aqueous solutions. The dotted line represents a purely non retarded inverse square van der Waals force law, inserted for comparison. Below ~6.5 nm the forces are effectively non retarded; above ~6.5 nm they decay more rapidly with increasing separation. $A = 2.2 \times 10^{-20}$ J. ●, 10^{-1} mol dm^{-3} KNO_3; ○, 1 mol dm^{-3} KNO_3; ■, 10^{-2} mol dm^{-3} $Ca(NO_3)_2$; □, 10^{-1} mol dm^{-3} $Ca(NO_3)_2$.

At smaller separations the surfaces often jump into molecular contact from a position (the " force barrier ") where the repulsion is maximum. By noting the position and force at the jump, an estimate may be made of the attractive force needed to bring about the jump into contact. Both methods require some extrapolation of the

repulsive forces. Those measurements in the regions of secondary minima generally yielded more accurate results, and provided detailed information of van der Waals forces in the range 4-15 nm. Measurements of jumps yielded less accurate results.

Fig. 10 shows data points obtained from 7 different experiments in which van der Waals forces were measured in the regions of secondary minima in 10^{-1} and 1 mol dm^{-3} KNO_3 (*cf.* fig. 4), as well as in 10^{-2} and 10^{-1} mol dm^{-3} $Ca(NO_3)_2$ solutions. For comparison the theoretical purely non retarded van der Waals force law $F/R = A/6D^2$, for a Hamaker constant of $A = 2.2 \times 10^{-20}$ J, has also been plotted (dotted line). The results may be summarized as follows:

(1) The van der Waals forces are largely independent of the type and concentration of electrolyte (in the range 10^{-2}-1 mol dm^{-3}), and of the strength and nature of the repulsive forces.

(2) The forces are non retarded up to about 6.5 nm, with a Hamaker constant of $A = (2.2 \pm 0.3)10^{-20}$ J. Results of jump measurements further indicate that the non retarded inverse square law of force extends down to below 1.5 nm separations, and that the effective force surface ($D = 0$ for the force) is within 0.2 nm of each mica–water interface.

(3) Above $\sim$6.5 nm retardation effects set in and the forces decay more rapidly with increasing separation.

(4) Measurement of the refractive index of water and aqueous solutions of KNO_3 and $Ca(NO_3)_2$ between two mica surfaces yielded values within 1 % of bulk values for surface separations in the range 2-100 nm. At separations below 2 nm the measuring accuracy falls, but the results do not indicate any deviations of the refractive indices from bulk values even when additional repulsive forces are present. We conclude that in theoretical calculations of van der Waals dispersion forces the bulk refractive indices should be adequate for calculations of these forces down to separations of 2 nm (and probably well below 2 nm).

We have not attempted to compare our results with theory, but we note that the van der Waals forces between two mica surfaces in aqueous solutions are much reduced in magnitude from those between mica surfaces in air, and that retardation effects set in earlier than they do in air.[46]

ADHESION STUDIES

When two mica surfaces are in adhesive contact (in a primary minimum) it is possible to measure the adhesion energy γ per unit area from the pull-off force P at which the surfaces jump apart:[48, 54]

$$P = 3\pi R\gamma. \tag{6}$$

The range of values we have obtained for the adhesive energies in aqueous electrolyte solutions ranged from $\sim$10 mJ m^{-2} to below 0.01 mJ m^{-2} (1 mJ m^{-2} = 1 erg cm^{-2}). In general, high γ values were measured whenever the additional repulsive forces were small. Our preliminary results indicate that the adhesive forces of mica surfaces in contact in a primary minimum are complex, and are not simply given by extrapolating the van der Waals and double-layer forces to separations of the order of inter-atomic spacings as is the case in some other systems.[55]

4. DISCUSSION

Silicates have long been known to exhibit unusual colloidal properties not accountable by current theories: many silicates swell spontaneously in aqueous solutions, and some show hysteresis; silica dispersions are sometimes stable at very

high electrolyte concentrations and undergo reversible coagulation, and the properties of water have often been found to be anomalous near silicate surfaces. These and other findings have led many to conclude that silicate and other oxide surfaces can induce structure on the water layers adjacent to them, though there has been a continuing controversy as regards the nature and extent of such water structuring effects. Our results may be viewed in two ways: at large separations, above about 7.5 nm, the measured forces have been close to those expected from the DLVO theory, and we may expect these results to apply more generally to other systems. At small separations, however, the forces have often deviated drastically from theoretical expectations, and here the results, and the conclusion drawn from them, may not be generally applicable to other systems. We shall now discuss the different aspects of our results in turn.

DOUBLE-LAYER FORCES

The double-layer forces in dilute KNO_3 solutions (10^{-4}-10^{-3} mol dm^{-3}) are in remarkably good agreement with theory at separations ranging from five Debye lengths down to below 0.2 Debye lengths. One important implication of these results is that the dielectric constant of water ε must be very close to the bulk value of 80 at separations down to at least 5 nm. Any significant deviation of ε from 80 would have shown up in the exponential slopes of the force curves. Thus these results may be interpreted as furnishing evidence that there is no significant water structuring at distances beyond 2.5 nm from each surface, and are in marked contrast to the results of Metsik *et al.*[38] and of Palmer *et al.*[56] who measured very low ε values for water layers between mica sheets, for example:[38] $\varepsilon = 8$ at $D = 100$ nm, and $\varepsilon = 4.5$ at $D = 70$ nm.

At higher KNO_3 concentrations (10^{-2}-10^{-1} mol dm^{-3}) the measured exponential decay lengths exceed the theoretical Debye lengths by about 25 %. Hough and Ottewill [24] have measured the pressure against distance dependence for two sodium dodecyl sulphate surfaces in 6×10^{-3} and 10^{-2} mol dm^{-3} 1 : 1 electrolyte solutions. Their measured exponential decay lengths were 1.35-1.39 of the theoretical values. This " agreement " with our value of 1.25 ± 0.15 in 10^{-2} mol dm^{-3} KNO_3 may reflect a general property of 1 : 1 electrolytes that their effective Debye lengths exceed the ideal values at high concentrations. If the Poisson–Boltzmann equation remains valid at these concentrations, then a glance at eqn (3) shows that either the aqueous dielectric constant ε must be higher than 80 or the effective concentration of free ions must be less than C. Most effects which are believed to influence ε, *e.g.*, electric field saturation, water structure, increased ionic strength, act to decrease rather than increase the value of ε.[52, 57] Thus an increased ε appears to be an unlikely explanation for the observed increase in the " experimental Debye lengths ". An alternative possibility is that the effective free ion concentration C is less than the total salt concentration, arising from ion-pairing of the Bjerrum type.[34]

The double-layer interaction in KNO_3 solutions occurs at, or very close to, constant potential both on approach of the two surfaces and on changing the electrolyte concentration. The potential is independent of pH in the range 5.5-7.0, but appears to be dependent on the chemical composition of the mica.

With the 2 : 1 electrolytes, $Ca(NO_3)_2$ and $BaCl_2$, the double-layer forces are much reduced from those in KNO_3 at the same concentration. Further, the exponential decay lengths are significantly *lower* than the theoretical Debye lengths already in dilute solutions (10^{-4}-10^{-3} mol dm^{-3}). These findings cannot be satisfactorily explained in terms of ion-pairing, electric field saturation, or deviations of the dielectric

constant of water from 80. The observed deviations may be related to the " structure breaking " and " structure promoting " effects that these ions have on water: thus KNO_3 is a " structure breaker ", while $BaCl_2$ and $Ca(NO_3)_2$ are " structure promoters ".[58]

HYSTERESIS AND STRUCTURAL ORDERING

We have found that the " force surface " or outer Helmholtz plane (OHP) is not necessarily at the mica water interface but may initially be as far as 2.5 nm beyond this interface. We use the term OHP in the conventional sense [39] as " the plane where diffuse double-layers starts, or the plane beyond which the charge distribution obeys Poisson–Boltzmann statistics ". Our conclusion that this plane may initially be ~2.5 nm beyond each surface is based on our many measurements of hysteresis where the only apparent explanation is that the OHPs are irreversibly shifted towards the surfaces on the first approach. Hysteresis effects have been previously observed in swelling pressure studies with aqueous dispersions of montmorillonite sheets in water and NaCl solutions.[25-27, 44] Our conclusion that hysteresis is due to a displacement of the OHPs establishes a definite link between the DLVO theory and any structured aqueous region at the mica surfaces. The location of the OHPs has always been difficult to establish. Lyklema [39] recently reviewed the state of the literature on AgI sols and concluded that the OHP is at ~0.54 nm beyond each surface and that this probably corresponds to the Stern layer thickness. He further concluded that there are no thick stagnant water layers at these interfaces. Bérubé and De Bruyn [59] have pointed out that the double-layers at AgI and Hg surfaces are very different from those at TiO_2 and other oxide surfaces, and proposed that long range range ordering of water, hydrogen bonded to oxide surfaces, may occur with a transition region between the ordered structure of this bound water and the differently organized bulk liquid. The location of this transition region is the most likely focal point for the establishment of the electrical double-layer. Webb *et al.*,[60, 61] in an attempt to further explain certain inadequacies in the DLVO theory regarding the dispersion stability of TiO_2 sols, later concluded that there exist immobilized or structured water layers 1.2-2.5 nm thick (5-10 molecular layers) near TiO_2 surfaces that physically control the locations of the hydrodynamic shear plane and the OHP. Quirk *et al.*[62, 63] reviewed the state of diffuse double-layer interactions as applied in the swelling of soil and other clay systems and concluded that only for surface separations >4 nm can diffuse double-layer theory be used to describe swelling. Posner and Quirk [64] measured the adsorption isotherms of water adsorbed from electrolyte solutions onto montmorillonite and illite and concluded that there exist ordered hydration regions on the surfaces which prevent electrolyte ions from reaching the mineral surfaces. It is also noteworthy that montmorillonite swelling appears to depend on the lattice *b*-dimension,[65] and that the surface lattice configurations of montmorillonites and micas closely match that of ice I (or water).

Our findings are consistent with these concepts. In KNO_3 solutions the Stern layer is at most 0.5 nm thick; beyond this there exists an aqueous region that is differently ordered from bulk water but whose refractive index is very close to that of bulk water. This region may extend 2.5 nm beyond each surface (or ~2.0 nm beyond the outer edge of the Stern layer), with the OHP being located at its outer boundary. When two mica surfaces approach each other the OHPs are irreversibly shifted towards the surfaces until they reach and then remain at the Stern layers, or very close to them. These shifts of the OHPs probably reflect the progressive collapse or breakdown of the structured aqueous regions as the surfaces

come together. The onset of the shifts of the OHPs occurs once they are sufficiently close to each other, and there are indications that the shifts usually commence once the repulsive *pressure* $\partial(F/2\pi R)/\partial D$ reaches $\sim 5 \times 10^4$ N m^{-2}, or ~ 0.5 atm. The existence and extent of such structured aqueous regions varies from mica to mica, and they, therefore, depend on the nature of the mica in addition to that of the electrolyte.

ADDITIONAL FORCES

We have found that additional repulsive forces are often present. These forces are in addition to the double-layer forces rather than a modification of double-layer forces, *i.e.*, they do not arise from a breakdown of the Poisson–Boltzmann equation. The additional forces are invariably exponential and have a decay length of 0.95 ± 0.20 nm. Their magnitude varies from mica to mica and is largely independent of electrolyte concentration and may also be independent of the type of electrolyte. They appear to be stronger whenever hysteresis effects are observed, though in $Ca(NO_3)_2$ no hysteresis was ever observed whereas large additional forces were. The maximum additional force measured was of order $F/R \approx 50\,000 \exp(-D/1.0\text{ nm})$ μN m^{-1}, corresponding to a pressure between two parallel plates of $10^7 \exp(-D/1.0\text{ nm})$ N m^{-2} or $100 \exp(-D/1.0\text{ nm})$ atm.

The effectiveness of these additional forces depends on the strength of the DLVO forces, but they are usually negligible above 7.5 nm separations. At high electrolyte concentrations these forces may determine the position and depth of the secondary minimum as well as that of the force barrier. At low electrolyte concentrations their influence may be negligible right down to the force barrier which is determined solely by DLVO forces. However, the additional forces do affect the adhesion energy of surfaces in contact in a primary minimum.

It is possible that the glue used to attach the mica sheets to the glass discs leaches out and adsorbs on the mica surfaces, and thus gives rise to the additional forces which would then be " steric stabilization " forces. Similar effects could arise from the adsorption of organic compounds from solution. The observation that these forces were always the same for similar mica surfaces, the absence of a time dependence of these forces, and the lack of correlation between the carbon content of the solution and the magnitude of these forces makes these explanations unlikely. On the other hand, we have not been able to find an obvious correlation between the strength of the additional forces, hysteresis, and the chemical composition of the mica sheets (we have yet to obtain X-ray data of the mica sheets). The finding that these forces are largely independent of the electrolyte concentration, and that their exponential decay length is invariably the same, strongly suggests that they are water structure (hydration) forces.[28, 36, 66]

VAN DER WAALS FORCES

Our results show that the van der Waals forces are non-retarded in the range 1-6.5 nm with a Hamaker constant of $(2.2 \pm 0.3) \times 10^{-20}$ J. Above 6.5 nm retardation effects set in and the forces decay more rapidly with increasing separation. The forces appear to be insensitive to changes in electrolyte concentration (below 1 mol dm^{-3}), and the " force surface " is at the mica–water interface to within 0.2 nm. We have not attempted to compare the results with theory, but there appear to be no indications of any serious discrepancies.

We thank R. J. Hunter, T. W. Healey, B. W. Ninham and D. J. Mitchell for valuable discussions, P. East for machining, N. G. Ware for electron microprobe assays, A. B. Howkins for help with carbon analysis, W. H. Steel for refractive index measurements, E. P. Honig and P. M. Mul for their computer program of double-layer interaction potentials, M. J. Scully for writing a new program, J. Gascoigne for technical assistance and R. K. Tandon for research assistance.

We particularly thank one referee for his thorough, constructive report.

APPENDIX 1

OPTICAL METHODS

The theory and use of multiple beam interferometry employing " fringes of equal chromatic order (FECO) " has been described before.[47]

If two back silvered sheets of mica of the same thickness T are in contact, and if white light is passed normally through them, the emerging light consists of discrete wavelengths $\lambda_n^0 (n = 1, 2, 3, \ldots,)$ which can be separated and measured as sharp fringes (FECO) in an ordinary prism or grating spectrometer. If the two mica surfaces are then separated by a distance D these fringes shift to longer wavelengths λ_n^D given by

$$\tan(2\pi\mu D/\lambda_n^D) = \frac{2\bar{\mu}\sin\left[\left(\frac{1-\lambda_n^0/\lambda_n^D}{1-\lambda_n^0/\lambda_{n-1}^0}\right)\pi\right]}{(1+\bar{\mu}^2)\cos\left[\left(\frac{1-\lambda_n^0/\lambda_n^D}{1-\lambda_n^0/\lambda_{n-1}^0}\right)\pi\right] \pm (\bar{\mu}^2-1)} \qquad \text{(A1)}$$

where + refers to odd order fringes (n odd), and − refers to even order fringes (n even). $\bar{\mu} = \mu_{\text{mica}}/\mu$, where μ_{mica} is the refractive index of mica at λ_n^D, and μ the refractive index of the medium between the two mica surfaces at λ_n^D.

By use of eqn (A1) both the distance D and the medium refractive index μ can be determined independently by measuring the shifts in wavelengths of an odd and an even fringe. The accuracy is about $\pm$(0.1-0.2) nm for measurements of D in the range 0-200 nm, while for μ it is better than 1 % at large D but is less accurate as D falls below 10 nm. To use eqn (A1) we only require an accurate prior determination of the refractive index of the mica. The refractive index and dispersion of our mica has been accurately measured by Dr. W. H. Steel of the Australian National Measurement Laboratory, CSIRO, Sydney, using standard Hg, Na and H spectral lines in the range 440-650 nm, who found for the γ and β components:

$$\mu_\gamma = 1.5846 + \frac{4.76\times10^5}{\lambda^2/\text{Å}}, \qquad \mu_\beta = 1.5794 + \frac{4.76\times10^5}{\lambda^2/\text{Å}}.$$

These values have been checked by us using an Abbé Refractometer (Carl Zeiss–Jena, Model G) using Hg and Na light. The accuracy is $\pm$0.0002—more than adequate for our purposes.

Note that the optical method for measuring the surface separation actually measures the distance between the two silvered layers on the reverse sides of the mica sheets. We have verified that no error greater than $\pm$0.1 nm in the surface separation is caused by normal temperature variations ($\pm$0.5°C) and applied pressures of the experiments.

CALIBRATIONS OF THE " CONTACT " POSITIONS ($D = 0$)

Tabor and Winterton [46] measured the thickness of a thin mica sheet after it had been partially cleaved, exposed to laboratory air (relative humidity 50-80 %) for 1 h, and then resealed. They compared this thickness to that of the uncleaved part of the sheet and found that it was 0.7 ± 0.2 nm thicker. They concluded that a 0.35 nm layer adsorbs onto a mica surface when it is exposed to air. We have performed similar measurements with some of our mica sheets and have found that the double thickness of the films adsorbed after 1 h exposure to air of relative humidity 40-45 % is 0.65 ± 0.15 nm (19 readings on three different mica sheets) in agreement with Tabor and Wintertons' value. For surfaces exposed to air for 3-5 h the adsorbed films were 0.85 ± 0.35 nm thick (0.4 ± 0.2 nm per surface). After exposure for 2 days the films were 2-3 nm thick. The refractive index of these adsorbed films was 1.8 ± 0.1.

During each force experiment the mica surfaces are always brought into molecular " contact " in air and the fringe positions noted; they are then separated and the box filled with liquid. This is usually done 3-5 h after the mica sheets are first exposed to air. We have invariably found that subsequent measurements of the contact positions in aqueous solutions (either in a primary minimum or under a large compressive force) occur 0.85 ± 0.30 nm farther in from those in air. Since this is exactly the thickness range of the adsorbed films after 3-5 h exposure to air, we conclude that (1) this film is water soluble, and that (2) " contact " in aqueous solutions occurs at 0.0 ± 0.4 nm relative to contact in uncleaved mica. It was generally observed that in $Ca(NO_3)_2$ solutions the contact positions of the primary minima were not affected by electrolyte concentration, nor by time (up to one day), to within ± 0.2 nm. In KNO_3 solutions, especially when large hysteresis effects or additional repulsions were observed, the contact positions tended to be a few Ångstroms farther out at higher electrolyte concentrations; this may be interpreted as indicating a progressive built up of the Stern layer with increased concentration.

APPENDIX 2

FORCE MEASURING TECHNIQUES

Fig. 11 shows a (force, distance) plot for two surfaces interacting *via* a hypothetical force law $F/R = 10\,000 \exp(D/a) - A \times 10^{24}/6D^2$ μN m^{-1}, where D is the distance of separation in nm, $a = 1$ nm, $R = 1$ cm, $A = 2.2 \times 10^{-20}$ J. If one of the surfaces is fixed while the other is suspended from a spring of stiffness K, then at equilibrium eqn (1) is satisfied. It may be shown that if $\partial F(D)/\partial D < K$ the equilibrium is stable, whereas if $\partial F(D)/\partial D > K$ it is unstable. Thus there exist certain instability regions in which no equilibrium is possible and where no forces may be measured. These regions are defined by $\partial F(D)/\partial D > K$, and, therefore, bounded by $\partial F(D)/\partial D = K$. The instability or excluded regimes are shown as dashed lines in fig. 11. If the two surfaces are brought up to these instability points, either on approach or separation, they will jump to new positions as indicated. For the hypothetical force law given above, and for a spring stiffness $K = 1.3 \times 10^2$ N m^{-1}, these instability points occur at $D = 0$ nm (jump from primary minimum contact), 1.5 nm (jump from force barrier into primary minimum contact), and at 6.1 and 8.4 nm (secondary minimum region). For the relatively low values of K used in our experiments the jumps into contact at the force barrier occur very close to where the force $F(D)$ actually peaks, *i.e.*, effectively at $\partial F(D)/\partial D = 0$. These jumps allow for accurate estimates of the magnitudes and positions of force barriers. On separating two

surfaces from contact in a primary minimum they usually jump apart a very large distance from which the pull-off force P may be readily obtained (see fig. 11). This in turn allows us to calculate the energy of adhesion as discussed in the text.

The right hand ordinate in fig. 11 gives the corresponding energy per unit area for two plane parallel surfaces, calculated according to the Deryaguin approximation [50] (energy/area $= F/2\pi R$). The second line in fig. 11 shows the equivalent force $\mathscr{F}$ between two plane surfaces interacting *via* the same force law, *viz.* $\mathscr{F} \propto \partial(F/2\pi R)/\partial D$. The force barrier has shifted from 1.5 to 2.0 nm, while the position of the secondary minimum (defined by $F = 0$ or $\mathscr{F} = 0$) has shifted from 3.5 to 5.3 nm. In general, for two planar surfaces the positions of the peaks in the repulsions (force barriers) or attractions (secondary minima) always occur farther out from those of two curved surfaces interaction *via* the same forces.

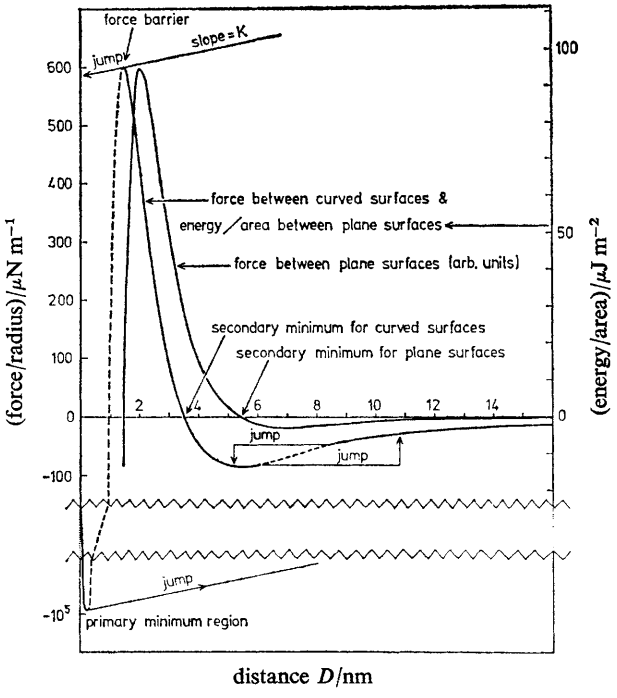

FIG. 11.—Left curve: Hypothetical force law for two crossed cylindrical surfaces of radius R: $F/R = 10\,000 \exp(D/a) - A \times 10^{24}/6D^2$ μN m^{-1}, where $a = 1$ nm, $R = 1$ cm, $A = 2.2 \times 10^{-20}$ J, showing positions of primary and secondary minima and the force barrier. If one of the surfaces is suspended from a spring of finite stiffness, $K = 1.3 \times 10^2$ N m^{-1}, there exist certain instability regimes, where no equilibrium is possible, shown as dashed lines. Right curve: law of force $\mathscr{F}$ for two planar surfaces interacting via the same forces (according to the Deryaguin approximation),[50] showing how the positions of the primary and secondary minima and the force barrier are shifted to larger distances.

Theoretical calculations of double-layer forces: Honig and Mul [67] have presented tables of the repulsive double-layer interaction energy of two plane parallel surfaces both at constant equal surface potential and at constant equal surface charge. Their results are exact solutions of the Poisson–Boltzmann equation for symmetrical electrolytes. Since the radii of the mica surfaces in our experiments ($R \sim 1$ cm) are much larger than the Debye lengths of the solutions ($\kappa R > 10^5$) the " Deryaguin

approximation " [50] may be assumed to hold. The interaction energy per unit area of two double-layers is then exactly equal to $F/2\pi R$. We are grateful to Drs. E. P. Honig and P. M. Mul for sending us their computer program, and to Mr. M. J. Scully who wrote out a new computer program in a different language, and who supplied us with many plots of theoretical double-layer forces. Scully's plots have been checked against those of Honig and Mul, and appear in many of the figures in the main text.

[1] B. V. Deryaguin and L. Landau, *Acta Phys. Chim. U.R.S.S.*, 1941, **14,** 633; *JETP* (*USSR*), 1945, **15,** 633.
[2] E. J. W. Verwey and J. Th. G. Overbeek, *Theory of the Stability of Lyophobic Colloids* (Elsevier, Amsterdam, 1948).
[3] J. Lyklema, in *Molecular Forces* (*Pontif. Acad. Sci. Scripta Varia*, North Holland, Amsterdam; J. Wiley Interscience, N.Y., 1967), vol. 31, p. 181, 221.
[4] D. H. Napper and R. J. Hunter, in *Hydrosols*, *MTP Int. Rev. Sci.*, *Surface Chem. and Colloids*, ed. M. Kerker, series 1, 1972, **7,** 241; series 2, 1975, **7,** 161 (Butterworth, London; University Park Press, Baltimore).
[5] J. Th. G. Overbeek, *J. Colloid Interface Sci.*, 1977, **58,** 408.
[6] I. E. Dzyaloshinskii, E. M. Lifshitz and L. P. Pitaevskii, *Adv. Phys.*, 1961, **10,** 165.
[7] J. Mahanty and B. W. Ninham, *Dispersion Forces* (Academic Press, London and New York, 1976).
[8] J. N. Israelachvili and B. W. Ninham, *J. Colloid Interface Sci.*, 1977, **58,** 14.
[9] J. N. Israelachvili and D. Tabor, *Prog. Surface Membrane Sci.*, 1973, **7,** 1.
[10] B. W. Ninham and V. A. Parsegian, *J. Theor. Biol.*, 1971, **31,** 405.
[11] D. Chan, T. W. Healy and L. R. White, *J.C.S. Faraday I*, 1976, **72,** 2844.
[12] V. A. Parsegian, *Ann. Rev. Biophys. Bioeng.*, 1973, **2,** 221.
[13] J. N. Israelachvili, *Quart. Rev. Biophys.*, 1974, **6,** 341.
[14] D. Gingell and I. Todd, *J. Cell Sci.*, 1975, **18,** 227.
[15] D. Gingell and J. A. Fornés, *Biophys. J.*, 1976, **16,** 1131.
[16] B. V. Deryaguin, A. S. Titijevskaia, I. I. Abricossova and A. D. Malkina, *Disc. Faraday Soc.*, 1954, **18,** 24.
[17] A. Scheludko and D. Exerowa, *Kolloid Z.*, 1960, **168,** 24.
[18] J. Lyklema and K. J. Mysels, *J. Amer. Chem. Soc.*, 1965, **87,** 2539.
[19] J. B. Rijnbout, W. A. B. Donners and A. Vrij, *Nature*, 1974, **249,** 242.
[20] G. Peschel and K. H. Aldfinger, *Z. Naturforsch.*, 1971, **26a,** 707; G. Schwarz, *Naturwiss.*, 1974, **61,** 215.
[21] B. V. Deryaguin, T. N. Voropayeva, B. N. Kabanov and A. S. Titiyevdkaya, *J. Colloid Interface Sci.*, 1964, **19,** 113.
[22] A. D. Roberts and D. Tabor, *Nature*, 1968, **219,** 1122.
[23] A. D. Roberts, *J. Colloid Interface Sci.*, 1972, **41,** 23.
[24] D. B. Hough and R. H. Ottewill, *Colloid and Int. Sci.*, *Hydrosols and Rheology*, ed. M. Kerker (Academic Press, N.Y., 1976), vol. IV, p. 45.
[25] L. M. Barclay and R. H. Ottewill, *Special Disc. Faraday Soc.*, 1970, **1,** 138.
[26] L. M. Barclay, A. Harrington and R. H. Ottewill, *Kolloid Z.*, 1972, **250,** 655.
[27] I. C. Callaghan and R. H. Ottewill, *Faraday Disc. Chem. Soc.*, 1974, **57,** 110.
[28] B. V. Deryaguin and N. V. Churaev, *J. Colloid Interface Sci.*, 1974, **49,** 249.
[29] A. D. Read and J. A. Kitchener, *J. Colloid Interface Sci.*, 1969, **30,** 391.
[30] F. M. Fowkes, *Ind. Eng. Chem.*, 1964, **12,** 40; *J. Colloid Interface Sci.*, 1968, **28,** 493.
[31] J. N. Israelachvili, *J.C.S. Faraday II*, 1973, **69,** 1729.
[32] J. Mahanty and B. W. Ninham, *J.C.S. Faraday II*, 1974, **70,** 637; *J. Chem. Phys.*, 1973, **59,** 6157.
[33] D. J. Mitchell and P. Richmond, *Chem. Phys. Letters*, 1973, **21,** 113; *J. Colloid Interface Sci.*, 1974, **46,** 118.
[34] R. A. Robinson and R. H. Stokes, *Electrolyte Solutions* (Butterworth, London, 2nd edn, 1959).
[35] B. V. Deryaguin, *Disc. Faraday Soc.*, 1966, **42,** 109.
[36] W. Drost-Hansen, *J. Colloid Interface Sci.*, 1977, **58,** 251.
[37] A. D. Bangham and D. R. Bangham, *Nature*, 1968, **219,** 1151.
[38] M. S. Metsik, V. D. Perevertaev and A. K. Lyubavin, in *Research in Surface Forces*, ed. B. V. Deryaguin (Consultants Bureau, N.Y. and London, 1975), vol. 4, section IV, p. 203, 217.
[39] J. Lyklema, *J. Colloid Interface Sci.*, 1977, **58,** 242.

[40] S. Marčelja and N. Radić, *Chem. Phys. Letters*, 1976, **42,** 129.
[41] S. Marčelja, D. J. Mitchell, B. W. Ninham and M. J. Sculley, *J.C.S. Faraday II*, 1977, **73,** 630.
[42] S. Marčelja, *Biochim. Biophys. Acta*, 1976, **455,** 1.
[43] J. N. Israelachvili and G. E. Adams, *Nature*, 1976, **262,** 774.
[44] K. Norrish and J. A. Raussell-Colom, *Clays and Clay Minerals*, 1963, **10,** 123.
[45] J. P. Friend and R. J. Hunter, *Clays and Clay Minerals*, 1970, **18,** 275.
[46] D. Tabor and R. H. S. Winterton, *Proc. Roy. Soc. A*, 1969, **312,** 435; J. N. Israelachvili and D. Tabor, *Nature*, 1972, **236,** 106; *Proc. Roy. Soc. A*, 1972, **331,** 19.
[47] J. N. Israelachvili, *Nature*, 1971, **229,** 85; *J. Colloid Interface Sci.*, 1973, **44,** 259.
[48] D. Tabor, *J. Colloid Interface Sci.*, 1977, **58,** 2.
[49] J. N. Israelachvili and D. Tabor, *Nature*, 1973, **241,** 112; *Wear*, 1973, **24,** 386.
[50] B. V. Deryaguin, *Kolloid-Z.*, 1934, **69,** 155.
[51] S. J. B. Reed and N. G. Ware, *X-Ray Spectr.*, 1973, **2,** 69; *J. Petrol.*, 1975, **16,** 499.
[52] J. B. Hasted, *Aqueous Dielectrics* (Chapman and Hall, London, 1973).
[53] V. A. Parsegian and D. Gingell, *J. Theor. Biol.*, 1972, **12,** 1192.
[54] K. L. Johnson, K. Kendall and A. D. Roberts, *Proc. Roy. Soc. A*, 1971, **324,** 301.
[55] J. Visser, *J. Colloid Interface Sci.*, 1976, **55,** 664.
[56] L. S. Palmer, A. Cunliffe and J. M. Hough, *Nature*, 1952, **170,** 796.
[57] J. Lyklema and J. Th. G. Overbeek, *J. Colloid Sci.*, 1961, **16,** 501.
[58] P. H. Von Hippel and T. Scheich, in *Structure and Stability of Biological Macromolecules*, ed. S. N. Timasheff and G. D. Fasman (Dekker, N.Y., 1969), pp. 417-574.
[59] Y. G. Bérubé and P. L. De Bruyn, *J. Colloid Interface Sci.*, 1968, **28,** 92.
[60] J. T. Webb, P. D. Bhatnagar and D. G. Williams, *J. Colloid Interface Sci.*, 1974, **49,** 346.
[61] P. D. Bhatnagar, *Colloid Interface Sci.*, ed. M. Kerker (Academic Press, 1976), vol. IV, p. 225.
[62] J. P. Quirk, *Israel J. Chem.*, 1968, **6,** 213.
[63] W. D. Kemper and J. P. Quirk, *Proc. Soil Sci. Soc. Amer.*, 1970, **34,** 347.
[64] A. M. Posner and J. P. Quirk, *Proc. Roy. Soc. A*, 1964, **278,** 35.
[65] I. Ravina and P. F. Low, *Clays and Clay Minerals*, 1972, **20,** 109.
[66] D. M. Le Neveu, R. P. Rand, V. A. Parsegian and D. Gingell, *Biophys. J.*, 1977, **18,** 209.
[67] E. P. Honig and P. M. Mul, *J. Colloid Interface Sci.*, 1971, **36,** 258.

(PAPER 7/1290)